Identical Partitioning of Consecutive Integer Set

Yimin D. Zhang † and Shunqiao Sun ‡

† Department of Electrical and Computer Engineering, Temple University, Philadelphia, PA 19122, USA
‡ Department of Electrical and Computer Engineering, The University of Alabama, Tuscaloosa, AL 35487, USA

Abstract—In this paper, we develop a scheme to partition a one- or multi-dimensional consecutive integer number set into multiple identical, possibly rotated, subsets. The proposed technique first exploits one-dimensional nested subsets, and the results are extended to achieve two- and multi-subset partitioning as well as in two- and multi-dimensional spaces. The number of consecutive lags in each case is examined. The results are useful to various sensing and communication applications, and sparse step-frequency waveform design for range estimation in automotive radar is demonstrated as an example.

Index Terms—integer set partition, multi-dimensional partition, sparse array, sparse waveform design, automotive radar

I. INTRODUCTION

The design and processing using sparse sensor arrays and sparse waveforms are a classical problem for effective system implementation with a lower complexity [1–4]. Nevertheless, the last decade witnessed significant interests and advancement in this direction [5–14]. This is motivated by the strong demands to pursue enhanced sensing capability, improved sensing accuracy, and increased communication capacity with a low complexity. Such progress was made possible due to the recent advancements in sparsity-based processing and convex optimization tools, such as compressive sensing and structured matrix completion [15–25].

In this context, sparse arrays and sparse waveforms are designed for a single user or a single platform to achieve the desired sensing performance subject to the complexity and cost constraints. In this paper, we consider the co-design of multiple sparse arrays or waveforms as a partition problem of a consecutive set, i.e., dividing a one-dimensional (1-D) or multi-dimensional (M-D) consecutive space into two or multiple non-overlapping subsets so that these subsets can be assigned to different users or platforms, or are used for different purposes, such as different functions in a multi-functional radar system.

Traditional array processing and spectral analyses often assume uniform space- and time-domain sampling as a result of Nyquist sampling. As such, the obtained data set are 1-D or M-D consecutive discrete sets. As sparse arrays and waveforms become more commonly used for effective data sampling and processing, various situations arise in which multiple sparse arrays and waveforms are designed as non-overlapping subsets of a consecutive integer set. For example, in random sparse step-frequency waveform design [26, 27], designing multiple non-overlapping step frequency sets would allow multiple radars to effectively share the entire spectrum band without mutual interference. Multiple frequency-diverse array (FDA) radars may use different sparse frequencies to achieve high range resolution with reduced interference [28, 29]. In massive multiple-input multiple-output (MIMO) systems, hybrid analog-digital systems may divide an array into multiple non-overlapping subarrays, and analog beam-forming is implemented in each subarray [30, 31]. Other applications include staggered synthetic aperture radar (SAR) using low-complexity sampling and inverse SAR (ISAR) exploiting sparse frequency bands and sparse apertures [32, 33]. Radar slow-times can also be partitioned into multiple subsets to be used by coordinated radar systems [34].

The focus of this paper is partitioning a full set into multiple identical, possibly rotated subsets, and each subset has consecutive different lags. Identical partition is desired for each subset to provide the same quality of service. In some problems, such as the the aforementioned analog beam-forming problem in a massive MIMO system, such structure would allow shared optimization among different subsets so that the optimization can be simplified. On the other hand, consecutive lags often make the subsequent signal processing more convenient and enable desired sensing performance, e.g., with low sidelobe levels. We adopt the simple nested configurations, which naturally partition a consecutive linear set into two identical but mirrored sparse segments. This concept is then extended into a two-dimensional (2-D) configuration to form four identical subsets. More general extensions to other dimensions and multi-subset partitioning are discussed. Sparse step-frequency waveform design for range estimation in automotive radar is demonstrated as an example.

Notations: We use lower-case (upper-case) bold characters to denote vectors (matrices). $(\cdot)^{\mathrm{T}}$ denotes the vector transpose, and $\mathrm{vec}(\cdot)$ represents the vectorization operation that turns a matrix into a vector by stacking all columns on top of one another. $|\mathbb{M}|$ denotes the cardinality of set $\mathbb{M}$, $\otimes$ and $\bigcup$ respectively denote the Kronecker product and union operators.

II. TWO-SUBSET 1-D PARTITIONING

Let $\mathbb{Q} = \{1, \cdots, Q\}$ be a 1-D set containing Q continuous integers between 1 and Q, where Q is assumed to be an even integer. Our objective is to partition $\mathbb{Q}$ into $G \geq 2$ subsets, i.e., $\mathbb{Q} = \mathbb{Q}_1 \cup \cdots \cup \mathbb{Q}_G$. We require that these subsets have identical, possibly rotated, patterns, and each subset, $\mathbb{Q}_g, g = 1, \cdots, G$, has consecutive difference lags which are desired to be as long as possible. In this paper, we consider a nested structure-based approach for systematical partitioning of 1-D or M-D partitioning, where the number of subsets in each dimension is an integer power of 2 (e.g., 2^K for some integer $K \geq 1$).
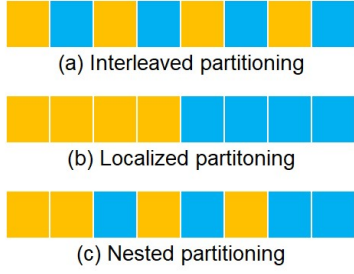
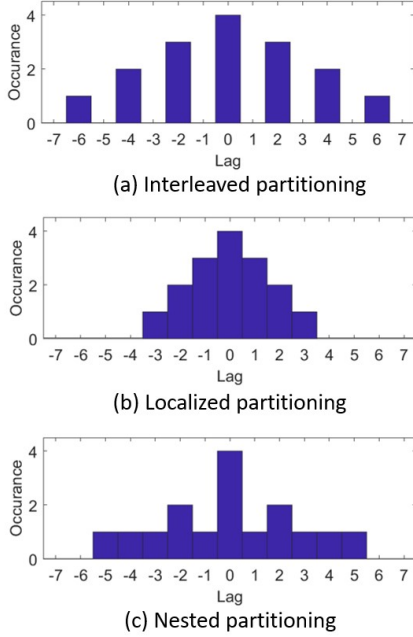Fig. 1: Three partitioning schemes of an 8-element set.

Fig. 2: Difference lags of the three partitioning schemes. Both subsets in each partitioning scheme share same difference lags.

A. Example of a 1-D Set Case

We start with a simple example where an 8-element consecutive set $\mathbb{Q} = \{1, \cdots, 8\}$ is portioned into $G = 2$ subsets. Fig. 1 depicts three possible patterns, which we respectively refer to as interleaved, localized, and nested. For the three partitions, the partitioning patterns are shown in Table I. It is clear that, for all three partitioning patterns, $\mathbb{Q}_1$ and $\mathbb{Q}_2$ are identical (interleaved and localized) or mirrored (nested).

The difference lag set for the gth subset is denoted as

$$\mathbb{Z}_g = \{z \mid z = u - v, u \in \mathbb{Q}_g, v \in \mathbb{Q}_g\}. \quad (1)$$

Fig. 2 shows the weight functions (number of occurrences) of the difference lags computed from these three pairs of subsets. For each pair, only one plot is shown because the two subsets result in identical difference lags. The interleaved

TABLE I: EXAMPLE OF 8-ELEMENT 1-D PARTITIONING

	Subset 1 $\mathbb{Q}_1$	Subset 2 $\mathbb{Q}_2$
Interleaved	$\{1, 3, 5, 7\}$	$\{2, 4, 6, 8\}$
Localized	$\{1, 2, 3, 4\}$	$\{5, 6, 7, 8\}$
Nested	$\{1, 2, 4, 6\}$	$\{3, 5, 7, 8\}$

partitioning uses a uniform undersampling pattern, thus leading to equally spaced gaps in the difference lags and causing alias. On the other hand, the localized partitioning provides consecutive lags, but the lags only extend between -3 and 3. The nested partitioning scheme becomes a preferred choice because it provides consecutive lags between -5 and 5.

B. General Rule for Two-Subset Partitioning

For two-subset partitioning, the first nested subset generally consists of two consecutive elements 1 and 2 as the inner group, followed by an arbitrary number of outer group elements separated by 2. Denoting the number of outer group elements as $N \geq 1$, the total number of elements in the first nested subset is $|\mathbb{Q}_1| = N + 2$, located at

$$\mathbb{Q}_1 = \{1, 2, 4, 6, \cdots, 2N, 2N + 2\}. \quad (2)$$

Similarly, the $|\mathbb{Q}_2| = N + 2$ elements of the second nested subset is located at

$$\mathbb{Q}_2 = \{3, 5, \cdots, 2N - 1, 2N + 1, 2N + 3, 2N + 4\}. \quad (3)$$

Both subarrays obtain consecutive difference lags between $-2N - 1$ and $2N + 1$. As such, the consecutive set $\mathbb{Q}$ is given as

$$\mathbb{Q} = \mathbb{Q}_1 \cup \mathbb{Q}_2 = \{1, 2, 3, \cdots, 2N + 3, 2N + 4\}, \quad (4)$$

which has $M = 2N + 4$ elements. It is clear that any consecutive integer set with an even number of elements can be partitioned into such nested subsets.

For the convenience of presentation in the sequel, we express the sets $\mathbb{Q}$ as all one vector $\boldsymbol{q} = \mathbf{1}_{(2N+4) \times 1}$, and define the following $(2N + 4) \times 1$ masking vectors for subsets $\mathbb{Q}_1, \mathbb{Q}_2$:

$$\boldsymbol{m}_g(k) = \begin{cases} 1, & \text{if } k \in \mathbb{Q}_g \\ 0, & \text{if } k \notin \mathbb{Q}_g, \end{cases} \quad (5)$$

for $g = 1, 2$.

III. MULTI-DIMENSIONAL PARTITIONING

In this section, we extend the two-subset 1-D partitioning results, discussed in Section II, into an M-D partitioning scenario, illustrated using the example of 2-D case. Consider a 2-D consecutive integer set $\mathbb{Q}$ of dimension $M^{[1]} \times M^{[2]}$ in the first (x) and second (y) directions, where $M^{[1]} = 2N^{[1]} + 4$ and $M^{[2]} = 2N^{[2]} + 4$. Note that $N^{[1]} \geq 1$ and $N^{[2]} \geq 1$ may take different values. We form a corresponding matrix $\boldsymbol{Q} = \mathbf{1}_{M^{[1]} \times M^{[2]}}$.

Following the same nested partitioning as described in Section II, we denote $\mathbb{Q}_g^{[1]}$ and $\mathbb{Q}_g^{[2]}$ as the gth nested subsets in the x- and y-directions, respectively, and their corresponding masking vectors are expressed as

$$\boldsymbol{m}_g^{[\eta]}(k) = \begin{cases} 1, & \text{if } k \in \mathbb{Q}_g^{[\eta]}, \\ 0, & \text{if } k \notin \mathbb{Q}_g^{[\eta]}, \end{cases} \quad (6)$$

for $\eta \in \{1, 2\}$ and $g \in \{1, 2\}$.

Now we form four 2-D subsets based on the outer product of $\boldsymbol{m}_{g_1}^{[1]}$ and $\boldsymbol{m}_{g_2}^{[2]}$ as g_1 and g_2 each takes a value of 1 or 2. We denote the resulting subset as

$$\boldsymbol{M}_{g_1, g_2} = \boldsymbol{m}_{g_1}^{[1]} \left(\boldsymbol{m}_{g_2}^{[2]} \right)^{\mathrm{T}}, \quad (7)$$
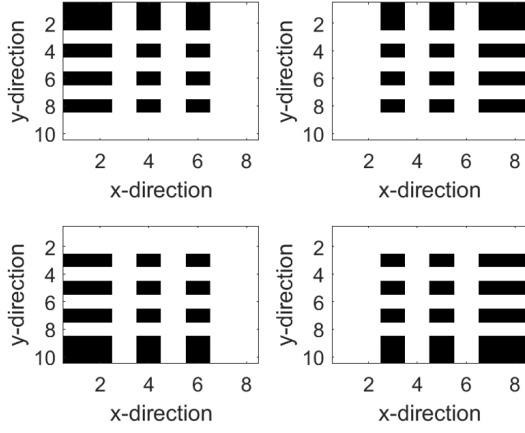
Fig. 3: Example of 2-D partitioning with $N^{[1]} = 2$ and $N^{[2]} = 3$. Black color indicates selection of elements.
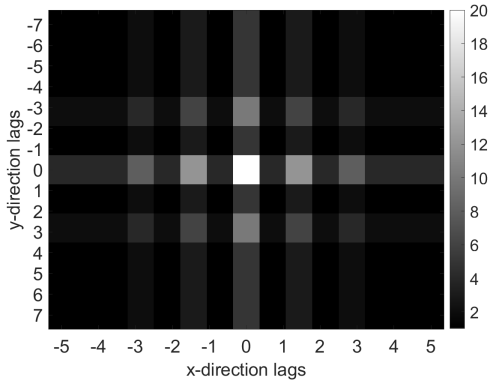

Fig. 4: Lag weights of the 2-D partitioning example.

where $g_1 \in \{1, 2\}$ and $g_2 \in \{1, 2\}$. Because they are derived from the 1-D nested partitioning scheme, it is straightforward to confirm that the difference lags of each subset is consecutive in $[-2N^{[1]} - 1 : 2N^{[1]} + 1, -2N^{[2]} - 1 : 2N^{[2]} + 1]$.

Fig. 3 shows an example of 2-D partitioning with $N^{[1]} = 2$ and $N^{[2]} = 3$, or equivalently $M^{[1]} = 8$ and $M^{[2]} = 10$. In this example, the element positions in each direction is shown in Table II, and the difference lags of each subset form a continue set in $[-5 : 5, -7 : 7]$. All the four subsets share the same lag weights that are depicted in Fig. 4. Note in this figure that the minimum value is 1, implying that all lags are filled.

Such nested partitioning strategies can be extended into high dimensions in a straightforward manner.

IV. SUPER-NESTED PARTITIONING

In the above 1-D and M-D partitioning, the number of subsets in each dimension is limited to two. In this section, we generalize the result to allow 2^K subsets in each dimension, where $K \geq 1$ may take different values for each dimension.

TABLE II: EXAMPLE OF 2-D PARTITIONING

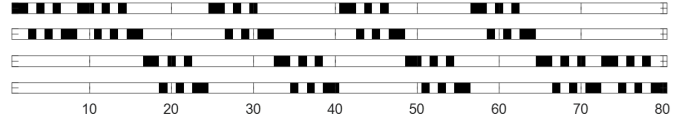|	Subset 1 $\mathbb{Q}_1^{[\eta]}$	Subset 2 $\mathbb{Q}_2^{[\eta]}$
x-direction 2	$\{1, 2, 4, 6\}$	$\{3, 5, 7, 8\}$
y-direction 1	$\{1, 2, 4, 6, 8\}$	$\{3, 5, 7, 9, 10\}$

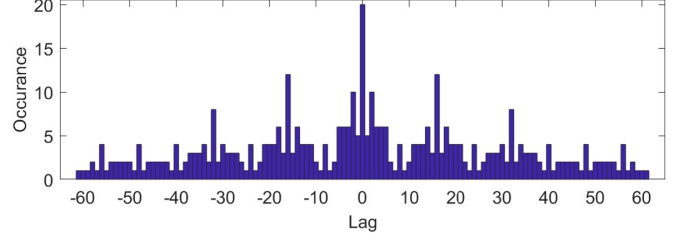Fig. 5: Example of four-subset 1-D partitioning. Black color indicate presence of elements.

Fig. 6: Difference lags of the four-subset 1-D partitioning.

Consider the vectorization of the 2-D partitioning problem considered in Section III. Vectorizing $\boldsymbol{M}_{g_1, g_2}$ becomes an $M^{[1]} M^{[2]} \times 1$ vector

$$\tilde{\boldsymbol{m}}_{g_1, g_2} = \text{vec}(\boldsymbol{M}_{g_1, g_2}) = \boldsymbol{m}_{g_2} \otimes \boldsymbol{m}_{g_1}, \qquad (8)$$

where $g_1 \in \{1, 2\}$ and $g_2 \in \{1, 2\}$.

This super-nested partitioning scheme exploits two layers of nested partitioning to obtain four subsets. The total number of elements in the full set is $(2N^{[1]} + 4)(2N^{[2]} + 4)$, and the number of elements in each of the four subsets is $(N^{[1]} + 2)(N^{[2]} + 2)$. The yielding difference lags are consecutive between $-(2N^{[1]} + 4)(2N^{[2]} + 1) - (2N^{[1]} + 1)$ and $(2N^{[1]} + 4)(2N^{[2]} + 1) + (2N^{[1]} + 1)$.

Corresponding to the 2-D partitioning example depicted in Section III, the four super-nested subsets are depicted in Fig. 5, and their common lag weights are shown in Fig. 6. Each subset has 20 elements, and the maximum lag in this case is 61.

Such super-nested partitioning approach can be easily extended to additional layers of Kronecker products in (8). Such results can also be used to construct 2-D and M-D partitioning by applying the super-nested subsets in Section III.

V. SIMULATION RESULTS

We demonstrate the proposed subset partitioning approach using an example that aims to perform unambiguous range estimation in an automotive radar. In this example, the frequency bandwidth is partitioned into multiple non-overlapping step-frequency subsets, thereby allowing multiple radar units to operate without mutual interference.

A step-frequency radar uses an equally spaced step-frequency waveform, where the available bandwidth B is divided into N_f frequency bins with a step frequency $f_\Delta = B/N_f$. As such, the frequency of the n_fth frequency bin is given as:

$$f_n = f_0 + (n_f - 1)f_\Delta, \quad n_f = 1, 2, \cdots, N_f, \qquad (9)$$

where f_0 is the base frequency. The synthetic range resolution obtained by coherently processing the return signal from a

(a) Interleaved pattern (b) Localized pattern (c) Partition pattern 1

(d) Partition pattern 2 (e) Partition pattern 3 (f) Partition pattern 4
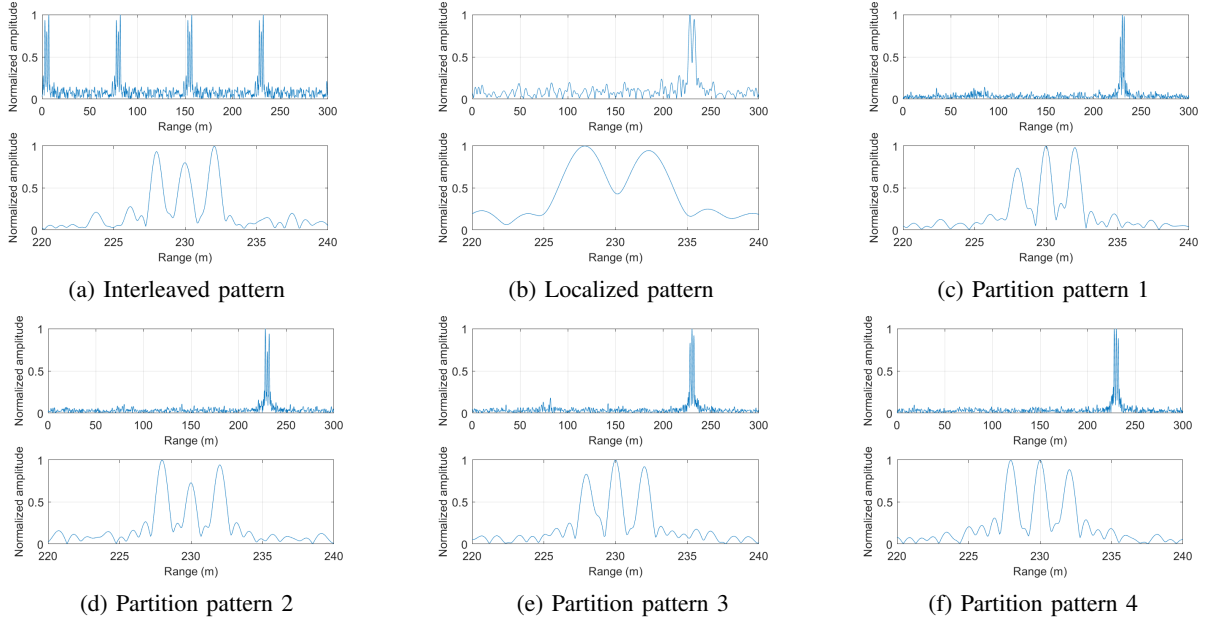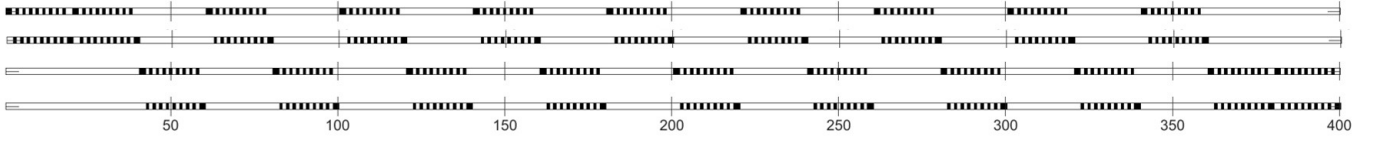
Fig. 7: Estimated range profile.

Fig. 8: Four partitioning patterns of the 400 step frequencies.

target corresponding to these N_f pulses is given as $\Delta R = c/(2B)$, and the maximum unambiguous range is given as $R_{\max} = c/(2f_\Delta)$.

Consider a radar system with a signal bandwidth of $B = 200$ MHz, which is divided into $N_f = 400$ step frequencies, rendering the step frequency to be $f_\Delta = 0.5$ MHz. When all the step frequencies are used by a single radar, the range resolution is $\Delta R = 0.75$ m, and the maximum unambiguous range is $R_{\max} = 300$ m.

Now we partition the 400 step frequencies into 4 orthogonal subsets. When the 1-D interleaved partitioning method is used, the maximum frequency span is approximately unchanged, but the step frequency will be increased to $4f_\Delta = 2$ MHz, thereby compromising the unambiguous range to 75 m. On the other hand, when the localized partitioning method is used, the step frequency and, subsequently, the unambiguous range are unchanged, but the bandwidth each waveform can use is reduced to only one-quarter of the full bandwidth, thus compromising the range resolution to 3 m.

Fig. 7 shows the estimated range profiles using different step frequency patterns where three point targets are located at ranges 227 m, 230 m, and 232 m. In each subplot, the top panel shows the range profile with the full range between 0 m and 300 m, and the bottom panel shows the enlarged result for range between 220 m and 240 m. Fig. 7(a) shows an aliased result obtained from an interleaved step frequency pattern, whereas Fig. 7(b) shows the unresolved result obtained from the localized step frequency pattern.

We propose the use of the super-nested 1-D partitioning scheme, described in Section IV, and each subset utilizes 100 step frequencies. We use $N^{[1]} = N^{[2]} = 8$ to construct the partitioning pattern, and the resulting partitioning patterns are shown in Fig. 8. In this case, the step frequency and thus the unambiguous range remain the same as $f_\Delta = 0.5$ MHz and $R_{\max} = 300$ m. On the other hand, the maximum frequency span of each waveform is 357 step frequencies, rendering the range resolution to be 0.84 m, which is only a 12% degradation from the original range resolution when all step frequencies are used.

Figs. 7(c) through 7(f) show the results obtained from the proposed four partitioned patterns, where 50 time samples are used to compute the correlation lags, and the targets are assumed to generate uncorrelated data samples. It is observed that the three targets are resolved without alias, and all four partitioned patterns yield similar performance.

VI. CONCLUSION

In this paper, we developed a scheme to partition a one- or multi-dimensional consecutive integer number set into multiple identical, possibly rotated, subsets. The usefulness was demonstrated using an example of sparse step-frequency waveform design for range estimation in an automotive radar. Such partitioning schemes are considered useful in various sensing and communication applications where sparse arrays and sparse waveforms are designed to share sensor and waveform resources by different platforms and functions.

VII. REFERENCES

[1] A. Moffet, "Minimum-redundancy linear arrays," *IEEE Trans. Antennas Propagat.*, vol. 16, no. 2, pp. 172–175, March 1968.

[2] R. T. Hoctor and S. A. Kassam, "The unifying role of the co-array in aperture synthesis for coherent and incoherent imaging," *Proc. IEEE*, vol. 78, no. 4, pp. 735–752, April 1990.

[3] X.-G. Xia and G. Wang, "Phase unwrapping and a robust Chinese remainder theorem," *IEEE Signal Process. Lett.*, vol. 14, pp. 247–250, April 2007.

[4] X. Li, Y. Zhang, and M. G. Amin, "Multifrequency-based range estimation of RFID tags," in *Proc. IEEE Int. Conf. RFID*, Orlando, FL, April 2009, pp. 147–154.

[5] P. P. Vaidyanathan, and P. Pal, "Sparse sensing with co-prime samplers and arrays," *IEEE Trans. Signal Process.*, vol. 59, no. 2, pp. 573–586, Feb. 2011.

[6] P. Pal and P. P. Vaidyanathan, "Nested arrays: A novel approach to array processing with enhanced degrees of freedom," *IEEE Trans. Signal Process.*, vol. 58, no. 8, pp. 4167–4181, Aug. 2010.

[7] S. Qin, Y. D. Zhang, and M. G. Amin, "Generalized coprime array configurations for direction-of-arrival estimation," *IEEE Trans. Signal Process.*, vol. 63, no. 6, pp. 1377–1390, March 2015.

[8] C. L. Liu and P. P. Vaidyanathan, "Super nested arrays: Linear sparse arrays with reduced mutual coupling–Part I: Fundamentals," *IEEE Trans. Signal Process.*, vol. 64, no. 15, pp. 3997–4012, Aug. 2016.

[9] A. Ahmed, Y. D. Zhang, and B. Himed, "Effective nested array design for fourth-order cumulant-based DOA estimation," in *Proc. IEEE Radar Conf. (RadarConf)*, Seattle, WA, May 2017, pp. 998–1002.

[10] J. Liu, Y. Zhang, Y. Lu, S. Ren, and S. Cao, "Augmented nested arrays with enhanced DOF and reduced mutual coupling," *IEEE Trans. Signal Process.*, vol. 65, no. 21, pp. 5549–5563, Nov. 2017.

[11] S. Qin, Y. D. Zhang, M. G. Amin, and B. Himed, "DOA estimation exploiting a uniform linear array with multiple co-prime frequencies," *Signal Process.*, vol. 130, pp. 37–46, Jan. 2017.

[12] Z. Zheng, W. Wang, Y. Kong and Y. D. Zhang, "MISC Array: A new sparse array design achieving increased degrees of freedom and reduced mutual coupling effect," *IEEE Trans. Signal Process.*, vol. 67, no. 7, pp. 1728–1741, April 2019.

[13] A. Ahmed and Y. D. Zhang, "Generalized non-redundant sparse array designs," *IEEE Trans. Signal Process.*, vol. 69, pp. 4580–4594, Aug. 2021.

[14] S. Zhang, A. Ahmed, Y. D. Zhang, and S. Sun, "Enhanced DOA estimation exploiting multi-frequency sparse array," *IEEE Trans. Signal Process.*, vol. 69, pp. 5935–5946, Oct. 2021.

[15] R. Tibshirani, "Regression shrinkage and selection via the Lasso," *J. Royal Statist. Soc.*, vol. 58, no. 1, pp. 267–288, 1996.

[16] D. L. Donoho, "Compressed sensing," *IEEE Trans. Inform. Theory*, vol. 52, no. 4, pp. 1289–1306, April 2006.

[17] J. A. Tropp and A. C. Gilbert, "Signal recovery from partial information via orthogonal matching pursuit," *IEEE Trans. Info. Theory*, vol. 53, no. 12, pp. 4655–4666, 2007.

[18] E. J. Candes and M. B. Wakin, "An introduction to compressive sampling," *IEEE Signal Process. Mag.*, vol. 25, no. 2, pp. 21–30, March 2008.

[19] S. Ji, D. Dunson, and L. Carin, "Multi-task compressive sampling," *IEEE Trans. Signal Process.*, vol. 57, no. 1, pp. 92–106, 2009.

[20] Q. Wu, Y. D. Zhang, M. G. Amin, and B. Himed, "Complex multitask Bayesian compressive sensing," in *Proc. IEEE Int. Conf. Acoust. Speech Signal Process. (ICASSP)*, Florence, Italy, May 2014.

[21] Y. Li and Y. Chi, "Off-the-grid line spectrum denoising and estimation with multiple measurement vectors," *IEEE Trans. Signal Process.*, vol. 64, no. 5, pp. 1257–1269, March 2016.

[22] C. Zhou, Y. Gu, X. Fan, Z. Shi, G. Mao, and Y. D. Zhang, "Direction-of-arrival estimation for coprime array via virtual array interpolation," *IEEE Trans. Signal Process.*, vol. 66, no. 22, pp. 5956–5971, Nov. 2018.

[23] C. Zhou, Y. Gu, Z. Shi, and Y. D. Zhang, "Off-grid direction-of-arrival estimation using coprime array interpolation," *IEEE Signal Process. Lett.*, vol. 25, no. 11, pp. 1710–1714, Nov. 2018.

[24] A. De Maio, Y. C. Eldar, and A. Haimovich (eds.), *Compressed Sensing in Radar Signal Processing*, Cambridge University Press, 2019.

[25] S. Liu, Z. Mao, Y. D. Zhang, and Y. Huang, "Rank minimization-based Toeplitz reconstruction for DoA estimation using coprime array," *IEEE Commun. Lett.*, vol. 25, no. 7, pp. 2265–2269, July 2021.

[26] K. V. Mishra, S. Mulleti, and Y. C. Eldar, "RaSSteR: Random sparse step-frequency radar," arXiv, https://arxiv.org/pdf/2004.05720.pdf, April, 2020.

[27] S. Sun and Y. D. Zhang, "4D automotive radar sensing for autonomous vehicles: A sparsity-oriented approach," *IEEE J. Sel. Top. Signal Process.*, vol. 15, no. 4, pp. 879–891, June 2021.

[28] S. Qin, Y. D. Zhang, M. G. Amin, and F. Gini, "Frequency diverse coprime arrays with coprime frequency offsets for multi-target localization," *IEEE J. Sel. Top. Signal Process.*, vol. 11, no. 2, pp. 321–335, March 2017.

[29] Z. Mao, S. Liu, Y. D. Zhang, L. Han, and Y. Huang, "Joint DoA-range estimation using space-frequency virtual difference coarray," *IEEE Trans. Signal Process.*, vol. 70, pp. 2576–2591, May 2022.

[30] J. Zhang, W. Liu, C. Gu, S. S. Gao, and Q. Luo, "Robust multi-beam multiplexing design based on a hybrid beamforming structure with nearly equal magnitude analogue coefficients," in *IEEE Trans. Vehi. Tech.*, vol. 71, no. 5, pp. 5564–5569, May 2022.

[31] J. Zhang, S. Li, L. Jin, W. Liu, and H. C. So, "Multi-beam multiplexing design with phase-only excitation based on hybrid beamforming architectures," in *Proc. IEEE Int. Conf. Acoust. Speech Signal Process. (ICASSP)*, Seoul, Korea, April 2024.

[32] M. Villano, G. Krieger, and A. Moreira, "Staggered SAR: High-resolution wide-swath imaging by continuous PRI variation," *IEEE Trans. Geosci. Remote Sens.*, vol. 52, no. 7, pp. 4462–4479, July 2014.

[33] G. Xu, B. Zhang, J. Chen, and W. Hong, "Structured low-rank and sparse method for ISAR imaging with 2-D compressive sampling," *IEEE Trans. Geosci. Remote Sens.*, vol. 60, pp. 1–14, 2022.

[34] L. Xu, S. Sun, K. V. Mishra, and Y. D. Zhang, "Automotive FMCW radar with difference co-chirps," *IEEE Trans. Aerosp. Electron. Syst.*, vol. 59, no. 6, pp. 8145–8165, Dec. 2023.